IEEE Access
Multidisciplinary ⋮ Rapid Review ⋮ Open Access Journal

Received July 30, 2018, accepted September 15, 2018, date of publication October 1, 2018, date of current version October 25, 2018.

Digital Object Identifier 10.1109/ACCESS.2018.2872791

A Fast and Efficient Method for the Composite Scattering of a Coated Object Above 3D Random Rough Surfaces

KE LI, LIXIN GUO, (Senior Member, IEEE), JUAN LI, AND SHUIRONG CHAI
School of Physics and Optoelectronic Engineering, Xidian University, Xi'an 710071, China

Corresponding author: Ke Li (xidian_keli@163.com)

This work was supported in part by the National Natural Science Foundation of China under Grant 61871457, Grant 61501360, Grant 61431010, and Grant 41806210 and in part by the Foundation for Innovative Research Groups of the National Natural Science Foundation of China under Grant 61621005.

ABSTRACT This paper presents a fast and efficient method that combines physical optics with physical optics to solve the composite scattering problem of a coated object above 3-D random rough surfaces. The object coated with lossy electric or magnetic radar absorbing materials is modeled as a stratified structure, and 3-D random rough surfaces are generated using Monte Carlo method with Gaussian spectrum. The proposed method utilizes fast and efficient physical optics as a solution for the coated object and the underlying random rough surface. Then a reradiation physical optics method based on Huyghens' principle is used as a solution for coupling scattering between the coated object and the underlying rough surface. The proposed method is numerically validated by comparing it with the commercial software FEKO and a multihybrid Kirchhoff approximation with the hybrid finite element-boundary integral algorithm. Runtime and memory consumption are also compared. Our method is found to reduce considerable time and memory while maintaining sufficient accuracy. The difference scattering radar cross section of a coated sphere above a 3-D perfectly electric conductor rough surface is numerically simulated. Furthermore, the dependence of difference scattering characteristic on the object coating parameters and the underlying rough surface parameters under different polarizations is discussed.

INDEX TERMS Composite scattering, coating object, rough surface.

I. INTRODUCTION

The composite electromagnetic (EM) scattering of an object above a rough surface is attracting the attention of many researchers. Accordingly, a wide range of composite EM scattering problems has been extensively analyzed in the past few decades. Composite EM scattering is an important and elementary class of problems in the field of EM simulations, and has extensive applications in long range radar surveillance, typical environmental remote sensing, target identification, target tracking [1]–[5]. Meanwhile, a perfect electric conductor (PEC) object coated with wave absorbing materials makes the composite problem complicated, because the coating materials can modify the target's radar cross section (RCS) [6]–[8], and they impose a remarkable influence on the composite scattering results.

Many numerical methods and their improved algorithms, such as the method of moments (MoM) [9], [10], extended propagation-inside-layer expansion combined with a forward-backward method scheme (EPILE-FBM) [11], generalized FBM with spectral acceleration algorithm [12], finite element method combined with a boundary integral method [13] and finite difference time domain method [14], have been investigated to numerically simulate the scattering from a composite model of a target and underlying rough surface. Meanwhile, various hybrid methods, such as the hybrid analytic method combined with MoM (KA-MoM) [15]–[17], algorithm that combines Kirchhoff approximation with the hybrid finite element-boundary integral (FE-BI-KA) [18], [19], and hybrid method that combines physical optics (PO) with PO [20]–[22], have been developed. Most of the abovementioned methods are first developed and used in 2D objects above a 2D rough surface. Subsequently, these methods or their improved algorithms, such as the parallel finite difference time domain approach [23], domain decomposition method-based scheme to improve traditional MoM solutions [24], 3D multilevel UV method [1], and extended propagation-inside-layer expansion combined with PO approximation (PO-EPILE) [3], have been developed as solutions for actual physical 3D objects above a 3D rough surface model. In addition, the problems of a coated object above rough surface are evaluated. Several methods, such as the auxiliary differential equation technique with FDTD (ADE-FDTD) [25] and a method that combines the reciprocity theorem with high-frequency approximation algorithm [26], can be found in the open literature. However, the scattering from the 3D composite model of coated object and rough surface is rarely reported. The 3D composite model of coated object and rough surface requires tremendous memory and CPU time. Meanwhile, details of electrically large dimensions make the 3D composite simulation a difficult task.

In this work, we proposed a fast and efficient method that combines PO with PO to solve the scattering of a coated object above 3D random rough surface. This method has been previously applied to 2D scattering problems related to a 2D PEC object above a 2D rough surface and its validity has been proven [20], [21]. The coated object in this study was modeled as a stratified structure. We considered the PO solution for a stratified patch. The interaction of an incident EM field with a non-perfectly conducting stratified patch on the object and perfectly conducting patch on the rough surface were described by Fresnel's reflection coefficients under different polarizations at the surface of the patch. A reradiation PO method based on Huyghens' principle was used as a solution for coupling scattering between the coated object and rough surface. The presented method was numerically validated by comparing it with the commercial software FEKO and a multihybrid FE-BI-KA algorithm [19]. The proposed method can remarkably reduce the memory and CPU time requirements.

The rest of this paper is organized as follows. Section 2 presents a detailed formula derivation of a coated object above randomly rough surface. Section 3 shows the numerical results and analyzes the dependence of difference scattering radar cross section (D-RCS) on object coating parameters and underlying rough surface parameters under different polarizations. Section 4 provides the conclusion and proposition on further investigation on this topic.

II. FORMULATION OF COMPOSITE SCATTERING

An infinite space is divided into two half spaces by a locally rough interface, and a rough surface is generated by using the Monte Carlo method [27], [28]. Fig. 1 shows the composite model of a coated sphere located in the upper space of the rough surface in the global coordinates of $Oxyz$. The rough surface is described as a function $z = f(x, y)$ where the average height is $< f(x, y) >= 0$, and is limited to a rectangular region $L \times L$ on $x - y$ plane of coordinate system in our numerical simulation. h is the altitude from the object center to $x - y$ plane. A plane wave impinges on the composite model with elevation angle θ_i and azimuth angle φ_i defined based on spherical coordinates, where $\hat{k}_i$ and $\hat{k}_s$ are the incident and scattering wave vectors. A general polarized incident wave can be decomposed into two linear polarized waves, namely, TE-polarized wave, which is perpendicular to the incident plane, and TM-Polarized wave, which is parallel to the incident plane. The incident plane is a plane determined by the incident wave vector and z axis in global coordinates. In this study, all fields and currents are assumed to have a time-harmonic dependence of the form $e^{-i\omega t}$, which is suppressed throughout this study. The rough surface and object are discretized into flat patches, and each patch has a different unit normal vector $\hat{n}$.

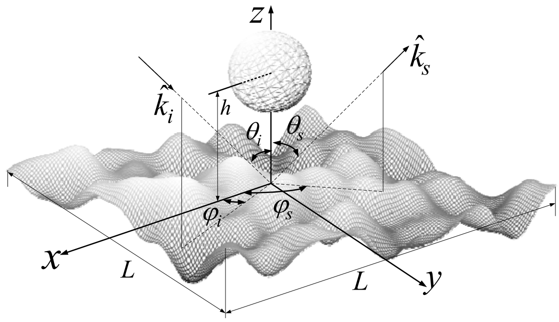

FIGURE 1. Geometry of an object above a rough surface.

In our previous work, the combined PO–PO method is established and used to calculate the scattering from a 2D object above 2D rough surface. This method separately calculates the EM scattering from an object and a rough surface and solves the mutual EM coupling between the object and surface by using a reradiation process based on PO currents. Similarly, the concepts are applicable to the scattering of a 3D object above a 3D rough surface. The multiple scattering processes can be found in [20] and [21], and multiple scattering models are depicted in Fig. 2.

Figure 2 illustrates the multiple scattering mechanisms of the composite model. Subscripts s and o denote the rough surface and object, the superscript number represents the order number of current, and they are the same for subsequent variables. The sketch map of scattering mechanisms shows the following conditions: the 1-order currents are induced on the object (rough surface) by the incident plane wave when the rough surface (object) is absent. The 1-order induced currents on the object (rough surface) radiate 1-order EM field which is regarded as the incident wave of the rough surface (object). Thus, the 2-order currents are induced and radiate the 2-order EM field. The 2-order EM field stimulates the next order current. The variables marked in black represent the primary currents. The variables marked in blue represent the secondary currents. The secondary currents are induced by the primary currents. The symbols in parentheses represent the radiation field of corresponding currents. Fig. 2 gives the currents up to 4-order, and high-order currents are omitted.

The direct scattering field of the object and rough surface is initially introduced for the 3D problem in this work.

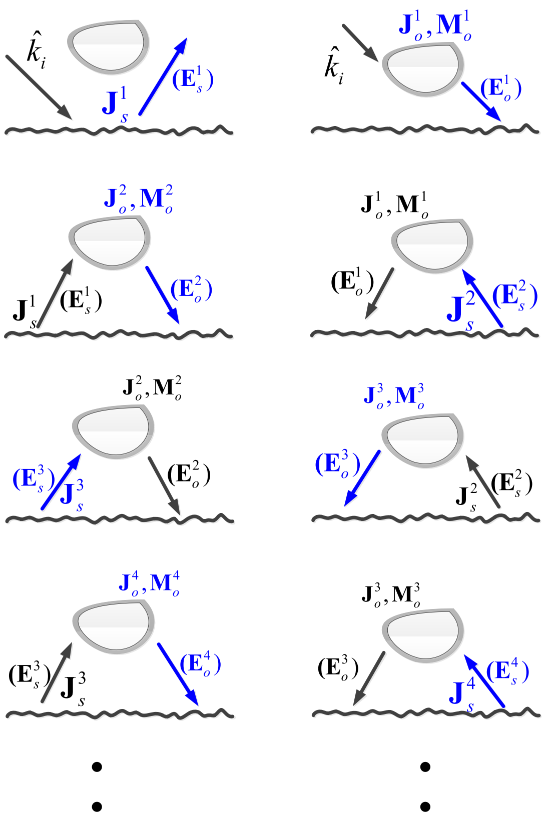

FIGURE 2. Multiple scattering models of coated object above rough surface.

The rough surface and object are discretized into flat patches, and an orthogonal local system coordinate *ouvn* is considered on an arbitrary flat patch. The local coordinate system is related to normal vector $\hat{n}$ on each discretized flat patch, and the unit vector components in the local coordinates can be expressed as

$$\hat{u} = \begin{cases} \hat{k}_i \times \hat{n}/|\hat{k}_i \times \hat{n}|, & (|\hat{n} \times \hat{z}| \neq 0) \\ \hat{x}, & (|\hat{n} \times \hat{z}| = 0) \end{cases}$$
$$\hat{v} = \hat{n} \times \hat{u} \tag{1}$$

For convenience, the incident wave is decomposed into transversal electric (TE) and transversal magnetic (TM) components in local coordinate *ouvn*, and the unit vectors in TE and TM components of the incident electric field can be defined as

$$\hat{e}_{TE} = \hat{u}, \quad \hat{e}_{TM} = \hat{e}_{TE} \times \hat{k}_i, \tag{2}$$

and the decomposition of the incident wave can be expressed as

$$\mathbf{E}^{inc} = \mathbf{E}^{inc}_{TE} + \mathbf{E}^{inc}_{TM} = \hat{e}_{TE} E^{inc}_{TE} + \hat{e}_{TM} E^{inc}_{TM}, \tag{3}$$

where $E^{inc}_{TE} = \mathbf{E}^{inc} \cdot \hat{e}_{TE}$ and $E^{inc}_{TM} = \mathbf{E}^{inc} \cdot \hat{e}_{TM}$ are the decomposed components of the incident electric field in the TE and TM vectors.

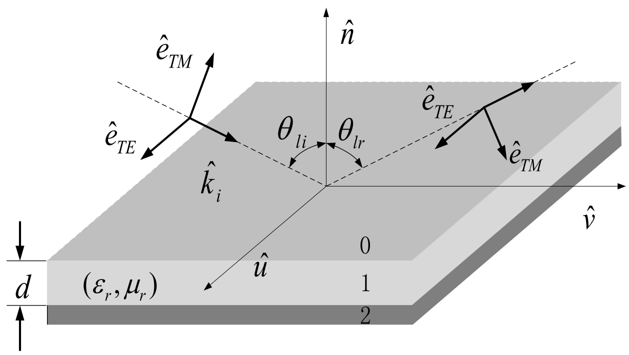

FIGURE 3. Planarity model of a coated PEC plane.

In this study, the coated object is modeled as a stratified structure, and the definition of local coordinates and the decomposition of the incident wave on the surface of the coated object is the same as (1) and (2). The PO solution is adopted for a stratified patch, and the surface field at the center of each patch is approximated as that of an infinite stratified plane by meeting the tangent plane approximation. The sketch map of the infinite plane coated with one-layer material is presented in Fig. 3. The space above the surface is "medium 0" (vacuum) with propagation vector $\mathbf{k_0} = k_{0u}\hat{u} + k_{0v}\hat{v} + k_{0n}\hat{n}$, the coated medium is "medium 1" with propagation vector $\mathbf{k_1} = k_{1u}\hat{u} + k_{1v}\hat{v} + k_{1n}\hat{n}$, and the perfectly conducting substrate is regarded as "medium 2."

Fig. 3 gives the incident and reflected waves in the incident plane based on Snell's law. The local incident angle and reflected angle are defined as

$$\cos\theta_{li} = -\hat{k}_i \cdot \hat{n}, \theta_{li} = \theta_{lr} \tag{4}$$

The interaction of an incident EM field with the plane can be described by local Fresnel's reflection coefficients R_{TE} and R_{TM} of TE and TM polarizations at the upper surface. When coated material constant (ε_r, μ_r) in medium 1 is known, the reflection coefficient at the surface of the plane in this study is expressed as [29]

$$R_{(TE/TM)} = \frac{1}{R_{01}} + \frac{[1-(1/R_{01}^2)]}{(1/R_{01}) + R_{12}\exp(-i2k_{1n}d)}, \tag{5}$$
$$R_{01} = (1-p_{01})/(1+p_{01}), \tag{6}$$

where $p_{01} = k_{1n}/(\mu_r k_{0n})$ for R_{TE} and $p_{01} = k_{1n}/(\varepsilon_r k_{0n})$ for R_{TM}. k_{0n} and k_{1n} are the longitudinal wave numbers in media 0 and 1 respectively. R_{12} is the reflection coefficient at the boundary of "medium 1" and "medium 2," and $R_{12} = -1$ for TE polarization and $R_{12} = 1$ for TM polarization based on the PEC surface boundary conditions. d is the thickness of the coated material. $R_{12} = 0$ and $d = 0$ are met without coating materials when the patch is a perfectly conducting surface. Then, $R_{(TE/TM)}$ can be degraded into R_{01}, and $R_{TE} = -1$ and $R_{TM} = 1$.

The object and the underlying rough surface are discretized, and the dimension of each discrete patch is less restricted than a wavelength. Thus, each order of current density is assumed to have constant amplitude and same phase distribution as that of the barycenter of each patch. On the basis of tangential plane approximation, the local reflection field of the flat patch can be obtained based on the different polarization components, and the equivalent surface electric and magnetic current densities can be written as

$$\mathbf{J} = \hat{n} \times \mathbf{H}(\mathbf{r}_c), \quad \mathbf{M} = \mathbf{E}(\mathbf{r}_c) \times \hat{n}, \tag{7}$$

where $\mathbf{r}_c$ is the position vector of each patch center. The PO equivalent current densities on the flat patches are zero in the non-lit region, and they are represented in the lit regions as follows [30]:

$$\begin{aligned}\mathbf{J} &= \frac{1}{\eta_0}[(1 - R_{TE})E_{TE}^{inc}(-\hat{n} \cdot \hat{k}_i)\hat{e}_{TE} \\ &\quad + (1 + R_{TM})E_{TM}^{inc}(\hat{n} \times \hat{e}_{TE})]|_s \\ \mathbf{M} &= [-(1 + R_{TE})E_{TE}^{inc}(\hat{n} \times \hat{e}_{TE}) \\ &\quad + (1 - R_{TM})E_{TM}^{inc}(-\hat{n} \cdot \hat{k}_i)\hat{e}_{TE}]|_s.\end{aligned} \tag{8}$$

Equation (8) can be used on the rough surface and object, and is the expression of 1-order currents $\mathbf{J}_s^1(\mathbf{J}_o^1, \mathbf{M}_o^1)$ induced by the incident wave on the rough surface or the object surface.

$$\begin{aligned}\mathbf{E}(\mathbf{r}) &= \int_s [i\omega\mu g(\mathbf{r}, \mathbf{r}')\mathbf{J} + \frac{i\omega\mu}{k^2}\nabla\nabla g(\mathbf{r}, \mathbf{r}') \\ &\quad \cdot \mathbf{J} - \nabla g(\mathbf{r}, \mathbf{r}') \times \mathbf{M}]ds \\ \mathbf{H}(\mathbf{r}) &= \int_s [i\omega\varepsilon g(\mathbf{r}, \mathbf{r}')\mathbf{M} + \frac{i\omega\varepsilon}{k^2}\nabla\nabla g(\mathbf{r}, \mathbf{r}') \\ &\quad \cdot \mathbf{M} + \nabla g(\mathbf{r}, \mathbf{r}') \times \mathbf{J}]ds.\end{aligned} \tag{9}$$

According to the Huygens' principle, the field at an observation point is expressed in terms of fields at the boundary surface, 1-order scattering field $\mathbf{E}_s^1(\mathbf{E}_o^1)$ from the rough surface or object can be obtained by substituting (8) to (9), $g(\mathbf{r}, \mathbf{r}')$ is the 3D scalar Green's function in "medium 0," and $g(\mathbf{r}, \mathbf{r}') = \exp(ikR)/(4\pi R)$, where $R = |\mathbf{r} - \mathbf{r}'|$ is the distance from source point $\mathbf{r}'$ to observation point $\mathbf{r}$.

Next, the radiation field is considered on the object surface from the rough surface. $\mathbf{J}_s^1$ is induced due to the incident wave calculated by (8). $\mathbf{J}_s^1$ radiates $\mathbf{E}_s^1(\mathbf{r}_o)$ on the object calculated by (9). Then $\mathbf{E}_s^1(\mathbf{r}_o)$ is regarded as the incident field of the coated object, and the 2-order induced currents $\mathbf{J}_o^2$ and $\mathbf{M}_o^2$ on the coated object can be obtained by the expression of (8) with the replacement of $\hat{k}_i$ by $\hat{r}_{so}$, All the definitions in (1)–(6) related to $\hat{k}_i$ must be replaced. $\hat{r}_{so}$ is the unit vector from the rough surface to the object, which is expressed as

$$\hat{r}_{so} = (\mathbf{r}_o - \mathbf{r}_s)/|\mathbf{r}_o - \mathbf{r}_s| \tag{10}$$

Once the 2-order induced currents $\mathbf{J}_o^2$ and $\mathbf{M}_o^2$ on the coated object are determined, its radiation field on the rough surface can be calculated by (9). The radiation field is

$$\begin{aligned}\mathbf{E}_o^2(\mathbf{r}_s) &= \int_s [i\omega\mu g\mathbf{J}_o^2 + \frac{i\omega\mu}{k^2}\nabla\nabla g \cdot \mathbf{J}_o^2 - \nabla g \times \mathbf{M}_o^2]ds_o \\ \mathbf{H}_o^2(\mathbf{r}_s) &= \int_s [i\omega\varepsilon g\mathbf{M}_o^2 + \frac{i\omega\varepsilon}{k^2}\nabla\nabla g \cdot \mathbf{M}_o^2 + \nabla g \times \mathbf{J}_o^2]ds_o.\end{aligned} \tag{11}$$

$\mathbf{E}_o^2(\mathbf{r}_s)$ is regarded as the secondary incident field of the rough surface, where $g = g(\mathbf{r}_s, \mathbf{r}_o)$ is the same as in (9).

On this basis, the 2-order current on the rough surface can also be obtained in an analogous means. The only difference is that the source and observation points are exchanged. The 2-order currents on the coated object and rough surface can be regarded as the secondary sources to calculate the 3-order currents when they are determined. The higher-order currents can be obtained by following this concept. Thus, the total currents on the coated object and rough surface can be expressed as

$$\begin{aligned}\mathbf{J}_o &= \mathbf{J}_o^1 + \mathbf{J}_o^2 + \mathbf{J}_o^3 + \mathbf{J}_o^4 + \cdots \\ \mathbf{M}_o &= \mathbf{M}_o^1 + \mathbf{M}_o^2 + \mathbf{M}_o^3 + \mathbf{M}_o^4 + \cdots \\ \mathbf{J}_s &= \mathbf{J}_s^1 + \mathbf{J}_s^2 + \mathbf{J}_s^3 + \mathbf{J}_s^4 + \cdots.\end{aligned} \tag{12}$$

In our simulation, the total currents will be convergent after a summation of several orders. In this study, the times of reradiation n are controlled by relative error functions [21], [31]

$$\varsigma_1 = |\mathbf{J}_o^n|/|\sum_{m=1}^{n}\mathbf{J}_o^m|, \quad \varsigma_2 = |\mathbf{M}_o^n|/|\sum_{m=1}^{n}\mathbf{M}_o^m|. \tag{13}$$

The relative error functions are set as $\varsigma_1 < 0.001$ and $\varsigma_2 < 0.001$. The reradiation between the coated object and rough surface is terminated when the two conditions on the coated object are met.

In this method, the propagation direction is regarded as the vector from the source point to observation point, as described in (10), when dealing with the coupling effects of coated object and underlying rough surface under high-order scattering simulations. The expressions of scalar Green's function and the operator acting on the scalar Green's function are substituted into (11). This process requires the PO validity that $(\mathbf{E}_o^2, \mathbf{H}_o^2, \hat{r}_{so})$ should meet right-handed helix relationship $\hat{r}_{so} \times \mathbf{E}_o^2/\eta_0 = \mathbf{H}_o^2$, that is, the local incident wave should meet the conditions of plane wave illumination. This condition is also discussed in the work of Ye and Jin [17]. In our numerical simulations, the condition is set as $h - R > 3.2\lambda$.

The bistatic D-RCS in this study is defined as [17], [19]

$$\sigma(\theta_s, \varphi_s; \theta_i, \varphi_i) = \lim_{R\to\infty} 2\pi R^2 \left\langle|\mathbf{E}_o^s + \mathbf{E}_s^s|\right\rangle. \tag{14}$$

$\mathbf{E}_o^s$ and $\mathbf{E}_s^s$ are the far zone scattering fields of the coated object and underlying rough surface, and they can be calculated by the first expression of (9). $\mathbf{E}_o^s$ is the result from $\mathbf{J}_o$ and $\mathbf{M}_o$, and $\mathbf{E}_s^s$ is the result from $\mathbf{J} = \mathbf{J}_s - \mathbf{J}_s^1$.

III. NUMERICAL RESULTS

In this section, the numerical results and analysis of EM scattering from a coated sphere above Gaussian rough surface are presented. The difference scattering of a coated PEC sphere above a PEC plane is initially calculated to validate our code. The D-RCS exposes the object scattering characteristics from the diffuse scattering of the underlying distributed source (the plane or rough surface) and reduces the dependency on the underlying surface. The difference scattering field is composed of the fields from the total currents on the object and coupling field from currents with 1-order current removed from the total currents on the underlying surface.

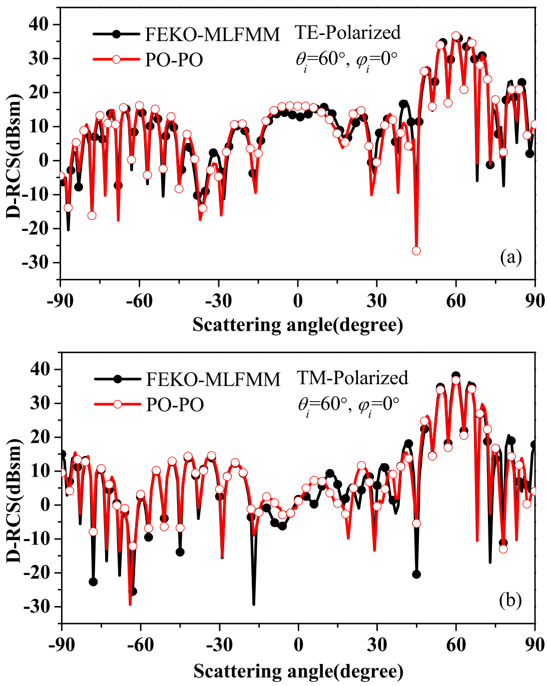

FIGURE 4. Comparison of D-RCS from a coated object above plane (a) TE-polarized (b) TM-polarized.

The bistatic difference scattering result of a coated sphere located above a PEC plane in incident plane (*xoz* plane) is shown in Fig. 4 under global TE and TM polarizations. The sphere has a radius of $r = 2\lambda$, coating thickness of $d = 0.1\lambda$, and relative dielectric constant of $\varepsilon_r = (2.0, 10.0)$, $\mu_r = 1.0$. The coating sphere has an altitude of $h = 6\lambda$ from the center to the plane. The incident waves are $\theta_i = 60°$ and $\varphi_i = 0°$. A truncated plane length $L = 100\lambda$ is adopted, and the results calculated by our method are compared with that obtained from the commercial software FEKO. The D-RCS is nearly coincident in most scattering directions, especially in the specular and backward scattering directions. As shown in Fig. 4, the results of the two different methods match well for most observation angles under different polarizations.

The scattering results of coated sphere above Gaussian rough surface are represented in the next examples. The PO method is also known as KA in the application of rough surface scattering [32]. The PO solution is effective when the curvature radii of rough surfaces meet the approximate condition, that is, the curvature radii are larger than the wavelength [29]. The profiles of rough surface are generated by Monte Carlo realizations with a Gaussian spectrum [33]. All the parameters of the rough surface in this study are set to meet the application conditions of PO. The coated object and incident wave parameters are the same as in Fig. 4 unless they are specifically stated. The simulated rough surfaces are PEC and $L = 100\lambda$. The scattering results are shown in incident plane (*xoz* plane), and the numerical results are determined by averaging 50 Monte Carlo realizations.

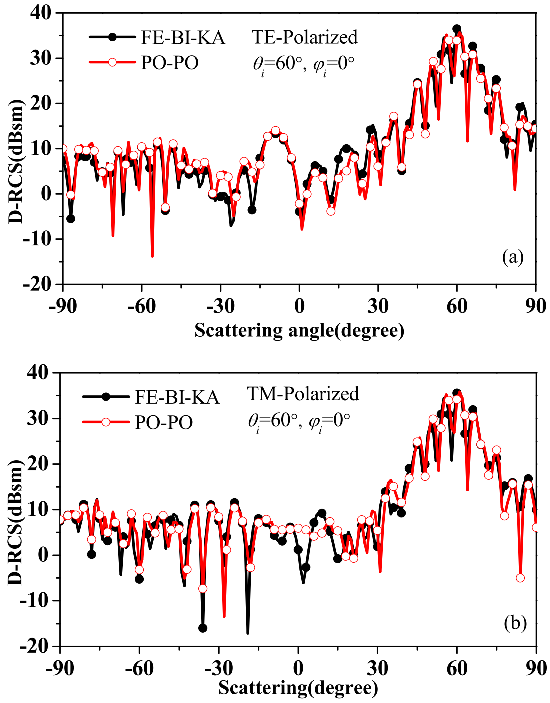

FIGURE 5. Comparison of D-RCS from a coated object above a rough surface (a) TE-polarized (b) TM-polarized.

To further show the validity of our method, D-RCS from a coated sphere above a rough surface by using our method is compared with that calculated by FE-BI-KA in reference [19] with only one Monte Carlo realization in Fig. 5. The plane in Fig. 4 is replaced by a rough surface in Fig. 5. For the rough surface, the root mean square (RMS) height is $\delta = 0.2\lambda$, and the correlation length is $l_x = l_y = l = 4.0\lambda$. As shown in Fig. 5, the results of the two different methods match well for most observation angles under different polarizations.

The D-RCS of the composite model for three coating EM parameters is compared under TE and TM polarizations in Fig. 6. The result without coating is marked in black, and the results coated with materials are marked in red and blued respectively. The coated materials are lossless medium with $\varepsilon_r = (2, 0)$, $\mu_r = 1$, and lossy medium with $\varepsilon_r = (2, 10)$, $\mu_r = 1$. The RMS height and correlation length are the same as in Fig. 5. Strong peaks appear, and small difference between them at specular directions is observed. This condition is because the presence of rough surface causes a strong specular scattering. Because the imaginary part of the dielectric constant of the coating layer represents loss, the presence of the coating layer can change the scattering results. Specifically, D-RCS remarkably decreases at directions away from the specular directions for lossy coating material.

The D-RCS of the composite model for different coating thicknesses under TE and TM polarizations is presented in Fig. 7. The coating thicknesses are set as $d = 0$

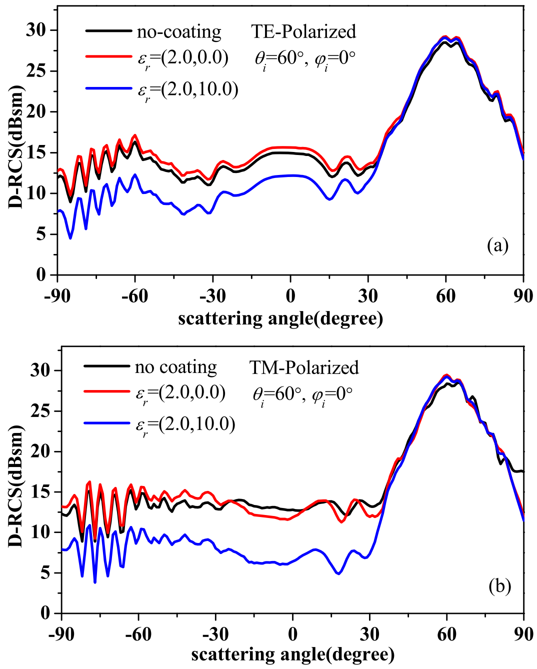

FIGURE 6. D-RCS for different coating EM parameters of an object above rough surface (a) TE-polarized (b) TM-polarized.

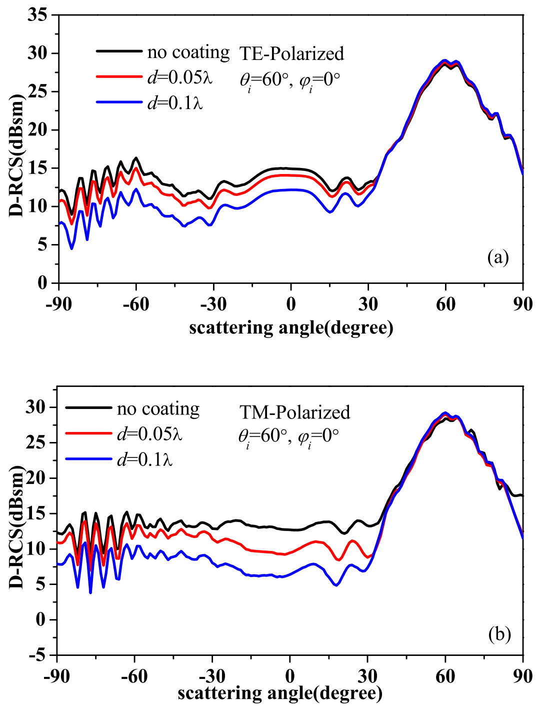

FIGURE 7. D-RCS for different coating thicknesses of an object above rough surface (a) TE-polarized (b) TM-polarized.

(no coating), 0.05λ and 0.1λ. The RMS height and correlation length are the same as in Fig. 5. Strong peaks appear, and small difference between the three curves at specular directions is observed. The underlying rough surface causes the strong specular scattering and is dominant near the specular directions. Meanwhile, the coating thicknesses have a limited impact on specular scattering. However, the change of thickness has remarkable influence on other directions apart from the specular directions. The D-RCS decreases with the increase of coating thickness. This condition is because the coating layer is lossy, and the scattering field is weakened with the increase of coating thickness.

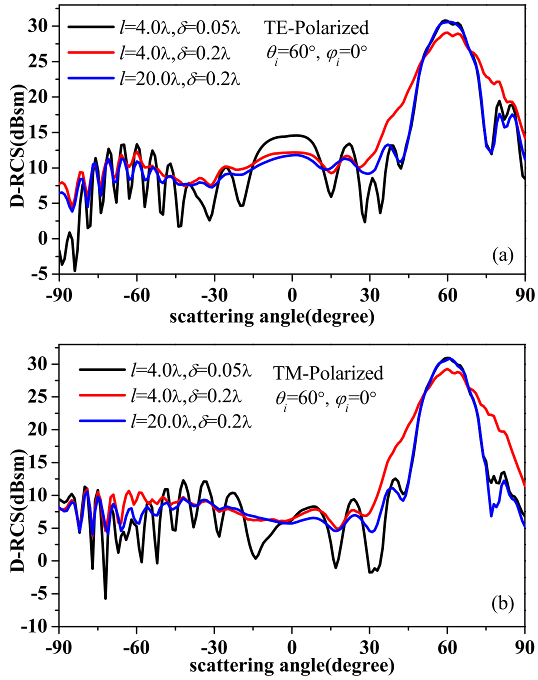

FIGURE 8. D-RCS for different roughness of a coated object above rough surface (a) TE-polarized (b) TM-polarized.

The D-RCS of the composite model for different surface roughness under TE and TM polarizations is presented in Fig. 8. Three combinations of Gaussian rough surface parameters are used with setting RMS height δ of 0.2λ and 0.05λ. Meanwhile, correlation length $l_x = l_y = l$ is set to 4λ and 20λ. The peak lobe is weak in specular directions and few oscillations exist in backward directions with the increase of RMS height. The peak lobe become strong in specular directions, and the effect on back scattering is relatively small with the increase of correlation length. The decrease of RMS height or increase of correlation length causes a rough surface to become smooth. Thus, the specular peak becomes strong and weak in other directions. The main peak lobe becomes narrow when the rough surface is smooth. This condition is because a smooth underlying rough surface can concentrate the scattering wave from the composite model. The influence of RMS height on the scattering results is obvious. However, the results show insensitivity to the change of correlation length.

Comparisons between the solution in this study with that in reference [19] are listed in Table 1 for the case of Fig. 5. The computer used on this study is a Windows Server 2008 R2 Enterprise 2.8 GHz PC with 128 GB memory.

TABLE 1. CPU time and required memory in Fig. 4.

Polarization	Method	CPU time	memory
TE-polarized	Proposed method	3.25 h	484.2 MB
	FE-BI-KA	6.58 h	10.02 GB
TM-polarized	Proposed method	3.27 h	484.2 MB
	FE-BI-KA	6.51 h	10.02 GB

The underlying rough surface is the same sample for the two methods, and the coated sphere is modeled by different approaches for the two methods. The coated sphere is modeled by the commercial software FEKO with 19376 flat patches for our method, and is modeled by the commercial software ANSYS with 41707 tetrahedrons for FE-BI-KA. The currents on the coated sphere are calculated by using an asymptotic method (PO) for our method, and it is calculated by using a numerical method (FE-BI) for FE-BI-KA. The coupling effect between the coated object and the underlying rough surface is calculated by considering an iterative process for our PO-PO method and the reference method FE-BI-KA. However, our method has fewer unknowns when calculating the scattering of coated object, and it does not need to solve the matrix as the FE-BI does. Therefore, the runtime and memory consumption are remarkably reduced for the two polarizations. Take TE polarization as an example, the runtime of the proposed method is 49.4% that of FE-BI-KA in reference, and the memory consumption is only 4.6% that of FE-BI-KA. This finding shows that the adopted method is fast and efficient.

IV. CONCLUSIONS

In this study, a PO–PO method is investigated for difference scattering of a coated object above 3D random rough surface. The PO method is used for the coated object and underlying rough surface, and the mutual coupling field between the coated object and rough surface is evaluated. The difference scattering due to the object presence above a plane is calculated to validate the proposed method. The proposed method remarkably reduces considerable runtime and memory consumption. Therefore, the proposed method is suitable in a stand-alone computer. Furthermore, the difference scattering of a coated sphere above Gaussian rough surfaces is numerically simulated. The model is calculated under different polarizations. The simulated results show that an increase of thickness of coating layer can reduce the D-RCS remarkably. The results under different surface roughness show that a smooth underlying rough surface can concentrate the scattering wave from the composite model. The influence of RMS height on the scattering results is obvious. However, the results show insensitivity to the change of correlation length.

REFERENCES

[1] F.-S. Deng, S.-Y. He, H.-T. Chen, W.-D. Hu, W.-X. Yu, and G.-Q. Zhu, "Numerical simulation of vector wave scattering from the target and rough surface composite model with 3-D multilevel UV method," *IEEE Trans. Antennas Propag.*, vol. 58, no. 5, pp. 1625–1634, May 2010.

[2] J. Li, B. Wei, Q. He, L. X. Guo, and D. B. Ge, "Time-domain iterative physical optics method for analysis of EM scattering from the target half buried in rough surface: PEC case," *Prog. Electromagn. Res.*, vol. 121, no. 1, pp. 391–408, 2011.

[3] M. Kouali, G. Kubicke, and C. Bourlier, "Electromagnetic interactions analysis between two 3-D scatterers using the E-PILE method combined with the PO approximation," *Progr. Electromagn. Res. B*, vol. 58, no. 58, pp. 123–138, 2014.

[4] L. Peng and Y. Q. Jin, "Numerical Simulation of the Doppler spectrum of a flying target above dynamic oceanic surface by using the FEM-DDM method," *Sci. China*, vol. 47, no. 5, pp. 597–612, 2004.

[5] H. Huang, L. Tsang, E. G. Njoku, A. Colliander, T.-H. Liao, and K.-H. Ding, "Propagation and scattering by a layer of randomly distributed dielectric cylinders using Monte Carlo simulations of 3D Maxwell equations with applications in microwave interactions with vegetation," *IEEE Access*, vol. 5, pp. 11985–12003, 2017.

[6] J.-J. Yao, S.-Y. He, Y.-H. Zhang, H.-C. Yin, C. Wang, and G.-Q. Zhu, "Evaluation of scattering from electrically large and complex PEC target coated with uniaxial electric anisotropic medium layer based on asymptotic solution in spectral domain," *IEEE Trans. Antennas Propag.*, vol. 62, no. 4, pp. 2175–2186, Apr. 2014.

[7] D. Colton and P. B. Monk, "Target identification of coated objects," *IEEE Trans. Antennas Propag.*, vol. 54, no. 4, pp. 1232–1242, Apr. 2006.

[8] H. Mosallaei and Y. Rahmat-Samii, "RCS reduction of canonical targets using genetic algorithm synthesized RAM," *IEEE Trans. Antennas Propag.*, vol. 48, no. 10, pp. 1594–1606, Oct. 2000.

[9] Y.-W. Wei, L.-X. Guo, A.-Q. Wang, and Z.-S. Wu, "Application of multiregion model to EM scattering from a dielectric rough surface with or without a target above it," *IEEE Trans. Antennas Propag.*, vol. 61, no. 11, pp. 5607–5620, Nov. 2013.

[10] H. Ye and Y.-Q. Jin, "Fast iterative approach to difference scattering from the target above a rough surface," *IEEE Trans. Geosci. Remote Sens.*, vol. 44, no. 1, pp. 108–115, Jan. 2006.

[11] Y. Liang, L.-X. Guo, Z.-S. Wu, and Q.-H. Liu, "A study of composite electromagnetic scattering from an object near a rough sea surface using an efficient numerical algorithm," *IEEE Antennas Wireless Propag. Lett.*, vol. 15, pp. 186–190, 2016.

[12] M. R. Pino, R. J. Burkholder, and F. Obelleiro, "Spectral acceleration of the generalized forward-backward method," *IEEE Trans. Antennas Propag.*, vol. 50, no. 6, pp. 785–797, Jun. 2002.

[13] L. X. Guo and R. W. Xu, "An efficient multiregion FEM-BIM for composite scattering from an arbitrary dielectric target above dielectric rough sea surfaces," *IEEE Trans. Geosci. Remote Sens.*, vol. 53, no. 7, pp. 3885–3896, Jul. 2015.

[14] J. Li, L. X. Guo, Y. C. Jiao, and K. Li, "Investigation on wide-band scattering of a 2-D target above 1-D randomly rough surface by FDTD method," *Opt. Express*, vol. 19, no. 2, pp. 1091–1100, 2011.

[15] H. Ye and Y. Q. Jin, "A hybrid analytic-numerical algorithm of scattering from an object above a rough surface," *IEEE Trans. Geosci. Remote Sens.*, vol. 45, no. 5, pp. 1174–1180, May 2007.

[16] S. Y. He and G. Q. Zhu, "A hybrid MM-PO method combining UV technique for scattering from two-dimensional target above a rough surface," *Microw. Opt. Technol. Lett.*, vol. 49, no. 12, pp. 2957–2960, 2007.

[17] H. Ye and Y.-Q. Jin, "A hybrid KA-MoM algorithm for computation of scattering from a 3-D PEC target above a dielectric rough surface," *Radio Sci.*, vol. 43, no. 3, pp. 1–15, Jun. 2008.

[18] J. Li, L. X. Guo, and Q. He, "Hybrid FE-BI-KA method in analysing scattering from dielectric object above sea surface," *Electron. Lett.*, vol. 47, no. 20, pp. 1147–1148, Sep. 2011.

[19] H.-J. He and L.-X. Guo, "A multihybrid FE-BI-KA technique for 3-D electromagnetic scattering from a coated object above a conductive rough surface," *IEEE Geosci. Remote Sens. Lett.*, vol. 13, no. 12, pp. 2009–2013, Dec. 2016.

[20] J. Li, L. Guo, and S. Chai, "Composite electromagnetic scattering from an object situated above rough surface," *Appl. Opt.*, vol. 53, no. 35, p. 8189, 2014.

[21] J. Li, L.-X. Guo, S.-R. Chai, and Y.-C. Jiao, "Electromagnetic scattering from a PEC object above a dielectric rough sea surface by a hybrid PO-PO method," *Waves Random Complex Media*, vol. 25, no. 1, pp. 60–74, 2015.

[22] K. Li, L. Guo, and J. Li, "Scattering and doppler spectral analysis for a fast-moving target above time-varying lossy dielectric sea surface," *Int. J. Antennas Propag.*, vol. 2016, Sep. 2016, Art. no. 8216309.

[23] L. X. Guo, J. Li, and H. Zeng, "Bistatic scattering from a three-dimensional object above a two-dimensional randomly rough surface modeled with the parallel FDTD approach," *J. Opt. Soc. Amer. A, Opt. Image Sci. Vis.*, vol. 26, no. 11, pp. 2383–2392, 2009.
[24] J. Chen, M. Wang, S. Li, X. Li, and M. Zhu, "A DDM-based scheme for analysis of electromagnetic scattering from target and rough surface composite model," *IEEE Antennas Wireless Propag. Lett.*, vol. 12, pp. 884–885, 2013.
[25] J. Li, L. X. Guo, Y. C. Jiao, and R. Wang, "Composite scattering of a plasma-coated target above dispersive sea surface by the ADE-FDTD method," *IEEE Geosci. Remote Sens. Lett.*, vol. 10, no. 1, pp. 4–8, Jan. 2013.
[26] R. Wang, S. R. Chai, and L. X. Guo, "Fast hybrid method for the study on monostatic scattering from plasma-coated target above a rough surface," *Int. J. Antennas Propag.*, vol. 2014, no. 4, 2014, Art. no. 762603.
[27] L. Tsang, J. A. Kong, and K. H. Ding, *Scattering of Electromagnetic Waves, Numerical Simulations*. New York, NY, USA: Wiley, 2001.
[28] Y. Kuga and P. Phu, "Experimental studies of millimeter-wave scattering in discrete random media and from rough surfaces—Summary," *Prog. Electromagn. Res.*, vol. 14, pp. 37–88, 1996.
[29] L. Tsang, J. A. Kong, and K. H. Ding, *Scattering of Electromagnetic Waves, Theories and Applications*. New York, NY, USA: Wiley, 2000.
[30] L. Tsang and J. A. Kong, *Scattering of Electromagnetic Waves, Advanced Topics*. Hoboken, NJ, USA: Wiley, 2004.
[31] W. Yang, Z. Zhao, C. Qi, W. Liu, and Z.-P. Nie, "Iterative hybrid method for electromagnetic scattering from a 3-D object above a 2-D random dielectric rough surface," *Prog. Electromagn. Res.*, vol. 117, pp. 435–448, Jun. 2011.
[32] N. C. Bruce and J. C. Dainty, "Multiple scattering from random rough surfaces using the Kirchhoff approximation," *J. Mod. Opt.*, vol. 38, no. 3, pp. 579–590, 1991.
[33] K. Pak, J. Johnson, L. Tsang, and C. H. Chan, "Backscattering enhancement of electromagnetic waves from two-dimensional perfectly conducting random rough surfaces based on Monte Carlo simulations," *J. Opt. Soc. Amer. A, Opt. Image Sci. Vis.*, vol. 12, no. 11, pp. 2491–2499, 1995.

KE LI received the B.S. degree in electronic information science and technology from Xidian University, Xi'an, China, in 2010, where he is currently pursuing the Ph.D. degree in radio science with the School of Physics and Optoelectronic Engineering, Institute of Radio Propagation. His research interests include applied and computational electromagnetics for remote sensing from target above or below random rough surfaces.

LIXIN GUO (S'95–M'03–SM'16) received the M.S. degree in radio science from Xidian University, Xi'an, China, in 1993, and the Ph.D. degree in astrometry and celestial mechanics from the Chinese Academy of Sciences, China, in 1999.

From 2001 to 2002, he was a Visiting Scholar with the School of Electrical Engineering and Computer Science, Kyungpook National University, Daegu, South Korea. He has been a Visiting Professor with the d'Energetique des Systemes et Precedes, University of Rouen, Mont-Saint-Aignan, France, and the Faculty of Engineering and Physical Sciences, University of Manchester, Manchester, U.K. He was a Distinguished Professor of Changjiang Scholars Program in 2014. He is currently a Professor and the Head of the School of Physics and Optoelectronic Engineering, Xidian University. He has been a Chief Professor of the Innovative Research Team in Shaanxi Province, China, since 2014. He has authored and coauthored four books and over 300 journal papers. He has been in charge of and undertaken over 30 projects. His research interests include electromagnetic wave propagation and scattering in complex and random media, computational electromagnetics, inverse scattering, and antenna analysis and design. He was the recipient of the National Science Fund for Distinguished Young Scholars in 2012.

JUAN LI received the B.S. degree from Shanxi University, Taiyuan, China, in 2005, and the Ph.D. degree in radio science from the School of Science, Xidian University, Xi'an, China, in 2010.

She is currently an Associate Professor with the School of Physics and Optoelectronic Engineering, Xidian University. Her research interests include fast algorithms for computational electromagnetics, scattering from complex target and rough surface, and wave propagation.

SHUIRONG CHAI received the B.S. degree and the Ph.D. degree in radio physics from Xidian University, Xi'an, China, in 2010 and 2016, respectively.

Since 2017, he has been a Post-Doctoral Researcher with the School of Physics and Optoelectronic Engineering, Xidian University. His current research interests include electromagnetic wave propagation and scattering in complex and random media, and computational electromagnetics.